Published in final edited form as:
J Hepatol. 2012 September ; 57(3): 549–555. doi:10.1016/j.jhep.2012.04.035.

Molecular MR Imaging of Liver Fibrosis: A Feasibility Study using Rat and Mouse Models

Miloslav Polasek[1,5], **Bryan C. Fuchs**[2,5], **Ritika Uppal**[1,4], **Daniel T. Schühle**[1], **Jamu K. Alford**[1], **Galen S. Loving**[1], **Suguru Yamada**[2], **Lan Wei**[2], **Gregory Y. Lauwers**[3], **Alexander R. Guimaraes**[1], **Kenneth K. Tanabe**[2], and **Peter Caravan**[1]

[1]A. A. Martinos Center for Biomedical Imaging, Department of Radiology, Massachusetts General Hospital and Harvard Medical School, 149 Thirteenth St., Suite 2301, Charlestown MA 02129

[2]Surgical Oncology, Massachusetts General Hospital Cancer Center and Harvard Medical School, WRN 401, 55 Fruit St., Boston, MA 02114

[3]Pathology, Massachusetts General Hospital and Harvard Medical School, WRN 2, 55 Fruit St., Boston, MA 02114

Abstract

Background & Aims—Liver biopsy, the current clinical gold standard for assessment of fibrosis, is invasive and has sampling errors, and is not optimal for screening, monitoring, or clinical decision-making. Fibrosis is characterized by excessive accumulation of extracellular matrix proteins including type I collagen. We hypothesize that molecular magnetic resonance imaging (MRI) with a probe targeted to type I collagen could provide a direct and non-invasive method for assessment of fibrosis.

Methods—Liver fibrosis was generated in rats with diethylnitrosamine and in mice with carbon tetrachloride. Animals were imaged prior to and immediately following i.v. administration of either collagen-targeted probe EP-3533 or non-targeted control Gd-DTPA. Magnetic resonance (MR) signal wash-out characteristics were evaluated from T1 maps and T1-weighted images. Liver tissue was subjected to pathologic scoring of fibrosis and analyzed for gadolinium and hydroxyproline.

Results—EP-3533 enhanced MR showed greater signal intensity on delayed imaging (normalized signal enhancement mice: control = 0.39±0.04, fibrotic = 0.55±0.03, p <0.01) and slower signal washout in fibrotic liver compared to controls (liver $t_{1/2}$ = 51.3±3.6 vs 42.0±2.5 min, p <0.05 and 54.5±1.9 vs 44.1±2.9 min, p <0.01 for fibrotic vs controls in rat and mouse models, respectively). Gd-DTPA enhanced MR could not distinguish fibrotic from control animals. EP-3533 gadolinium concentration in liver showed strong positive correlations with hydroxyproline levels (r = 0.74 (rats), r = 0.77 (mice)) and with Ishak scoring (r = 0.84 (rats), r = 0.79 (mice)).

Conclusion—Molecular MRI of liver fibrosis with a collagen-specific probe identifies fibrotic tissue in two rodent models of disease.

Contact information: Peter Caravan, A. A. Martinos Center for Biomedical Imaging, Department of Radiology, Massachusetts General Hospital and Harvard Medical School, 149 Thirteenth St., Suite 2301, Charlestown MA 02129. Phone: 1-617-643-0193, fax: 1-617-726-7422, caravan@nmr.mgh.harvard.edu.
[4]Current address: GE Healthcare, Medical Diagnostics, Bangalore, India
[5]Contributed equally to this work

Conflict of interests: P.C. has >5% equity in Collagen Medical, LLC, a company working to commercialize the MRI probe used in this study. All other authors have no conflicts.

Keywords

Molecular Imaging; Gadolinium; Type I Collagen; Carbon Tetrachloride; Diethylnitrosamine

Introduction

The liver possesses a unique ability to regenerate from a variety of injuries. Depending on the extent and duration of the injury, the healing processes may result in scarring (fibrosis) of the liver parenchyma. At the microscopic level this is observed as an accumulation of extracellular matrix (ECM) rich in fibrillar collagen, mainly types I and III [1]. Long-lasting, chronic insults such as hepatitis B or C virus infections, obesity, diabetes, alcohol abuse and other toxic insults all trigger cellular and molecular events that lead to liver fibrosis [2, 3]. The progression is typically slow and it may take decades to accumulate significant fibrosis in the liver. However, untreated fibrosis is likely to further progress into cirrhosis, which imposes a high risk of hepatocellular carcinoma and/or liver failure [4, 5]. Rising levels of obesity and diabetes, the spread of hepatitis B and C infections, and other factors have put millions of people worldwide in danger of developing cirrhosis [6–8].

Liver fibrosis is currently recognized as a dynamic process with a high potential for partial or complete resolution, provided that the underlying cause of the disease is suppressed or removed [1, 9]. One key element in an efficient treatment is a reliable diagnostic method that allows accurate staging of fibrosis to follow disease progression or response to therapy. Liver biopsy is the gold standard for staging of liver fibrosis [10]. However, it remains an imperfect method with appreciable sampling error [11, 12], high inter-observer variability, and is associated with risk of complications: hospitalization is required in 1 – 5 % of cases and mortality rate is between 0.01 and 0.1 % [13, 14]. Liver biopsy is also an invasive and painful procedure and repeated tests are often encountered with low patient compliance. Therefore, there is an urgent need for a reliable diagnostic method for non-invasive assessment of liver fibrosis [10, 15–18]. Several methods based on serum biomarkers have been reported that can identify fibrosis, however these are generally unreliable when it comes to staging of the disease [10]. Transient elastography [19–22] and magnetic resonance elastography [23–26] are methods that measure stiffness of the liver associated with fibrosis. Both methods reliably detect moderate and advanced fibrosis but diagnostic accuracy is lower for milder stages of disease and test performance may be low in patients with ascites or morbid obesity [19].

Over-expression of collagen is a hallmark of liver fibrosis. Here we hypothesized that molecular magnetic resonance imaging (MRI) with a probe targeted to type I collagen could provide a non-invasive method for assessment of fibrosis. EP-3533 is a gadolinium-based probe designed to specifically target type I collagen [27] that has previously demonstrated its utility in MRI of cardiac fibrosis [28]. The goal of this study was to assess the feasibility of EP-3533 to quantify liver collagen and determine whether collagen targeted MRI has the potential to act as a non-invasive measure of liver fibrosis.

Materials and methods

Animal models

All experiments were performed in accordance with the NIH Guide for the Care and Use of Laboratory Animals and were approved by the institution’s animal care and use committee. Male Wistar rats (Charles River Laboratories, Wilmington, MA) were given weekly intraperitoneal injections of 100 mg/kg diethylnitrosamine (DEN; Sigma, St. Louis, MO) for 4 weeks (n=5). Control animals received PBS (n=4). Strain A/J male mice (Jackson

Laboratories, Bar Harbor, ME) were administered 0.1 mL of a 40% solution of carbon tetrachloride (CCl4; Sigma) in olive oil by oral gavage three times a week for 20 weeks (n=8); age matched controls received only pure olive oil (n=4), or no vehicle (n=6). Animals from both models were imaged one week after the last injection to avoid acute effects of DEN or CCl4.

Probes

EP-3533 comprises a ten amino acid cyclic peptide conjugated to three gadolinium moieties, and was synthesized as previously reported [27]. The peptide confers affinity for type I collagen (Kd=1.8 μM) and the gadolinium moieties provide strong signal enhancement (relaxivity = 16.2 $mM^{-1}s^{-1}$ (5.4 per Gd ion) at 4.7T) [27, 28]. The commercial extracellular contrast agent gadopentetate dimeglumine (Gd-DTPA, relaxivity = 3.8 $mM^{-1}s^{-1}$ at 4.7T) was used as a control [29].

MR imaging and analysis

Animals were anesthetized with isoflurane (1–2%) and placed in a specially designed cradle with body temperature maintained at 37 °C. The tail vein was cannulated for intravenous (i.v.) delivery of the contrast agent while the animal was positioned in the scanner. Imaging was performed at 4.7 T using a small bore animal scanner with a custom-built volume coil. Doses of the contrast agents were chosen to yield similar signal enhancement based on relaxivity: 100 μmol/kg (Gd-DTPA) and 20 μmol/kg (EP-3533).

The imaging paradigm was similar for rats and mice. A series of baseline images were acquired, a bolus of Gd-DTPA was administered i.v. and the imaging was repeated for a period of 60 minutes post injection. Animals were then returned to their cages and imaged again 24 hrs (mice) or 48 hrs (rats) later. In the second imaging session, baseline images were again acquired followed by bolus injection of EP-3533, and imaging was repeated for 60 minutes. Following the second imaging session, animals were euthanized (120 minutes post injection for rats, 80 minutes post injection for mice), and liver and other tissues were removed for further analysis.

The imaging protocol involved a T1-mapping sequence (RARE inversion recovery (IR), TR/TE=3200ms/4ms, matrix=128×128, 7 or 8 inversion times from 7 to 3000 ms, single slice (2 mm for rats, 1 mm for mice), RARE factor 8) that was performed prior to and at 5 or 6 time points out to 60 min post injection. These sequences were alternated with a T1-weighted sequence (rats: IR-RARE with inversion time chosen to null the liver signal at baseline, TR/TE=3200ms/4ms, matrix=128×128, three 2 mm slices, 2 averages, RARE factor 8, acquisition time = 1.9 min; for mice: gradient echo (TR/TE/flip angle =50ms/1.92ms/35°, matrix=72×72 interpolated to 128×128, five 1mm thick slices). For the mouse studies an additional dynamic contrast enhanced (DCE) study was added. The same gradient echo sequence was run from 1.5 min pre- to 4.5 min post-injection with 3.6s temporal resolution. FOV=7.2×7.2 cm for rats and 3.6×3.6 cm for mice.

T1 was quantified from a 3 parameter fit of the dependence of liver signal intensity (SI) on inversion time (TI) using Microsoft Excel with Solver software, equation 1.

$$SI = SI_0[1 - Ae^{-TI/T1} + e^{-(TR+TI)/T1}] \quad (1)$$

Here TR is the repetition time, SI_0 is signal intensity at full recovery, and A is a preexponential factor. T1, SI_0, and A were iteratively varied to fit the observed data.

Liver $t_{1/2}$ values were estimated by fitting the change in ΔR1 values ($\Delta R1=1/T_{1,post}-1/T_{1,pre}$) with time, assuming a mono-exponential decay.

The DCE data were normalized to maximum enhancement (as 100%) to compare curves across animals.

Tissue analysis

Formalin-fixed samples were embedded in paraffin, cut into 5 μm-thick sections and stained with Masson's trichrome (rats) or Sirius red (mice) according to standard procedures. Trichrome and Sirius red stained sections were analyzed to score the amount of liver disease according to the method of Ishak [30]. Additional sections were stained with an antibody specific for collagen type I (Abcam, Cambridge, MA) with detection by an appropriate secondary antibody according to the manufacturer's instructions. All slides underwent blinded review by a board certified pathologist with expertise in gastrointestinal and hepatic malignancies. Hydroxyproline in tissue was quantified by HPLC analysis using a reported method [31]. Gadolinium was quantified in tissue acid digests by inductively coupled plasma-mass spectrometry (ICP-MS) using dysprosium as an internal standard. Hydroxyproline and gadolinium are expressed as amounts per wet weight of tissue. Gadolinium concentrations in the mouse livers were normalized to the gadolinium concentration in blood to compensate for variations in the injected doses.

Real-time *PCR*

Real-time PCR was performed on liver samples from a separate set of animals that were not imaged but received the exact same treatment as the imaged animals. Total RNA was extracted from liver tissue using TRIzol (Invitrogen, Carlsbad, CA) according to the manufacturer's instructions and subsequently treated with DNase I (Promega, Madison, WI). 250 ng of total RNA from each sample was used to create cDNA by single strand reverse transcription (SuperScript III First-Strand Synthesis SuperMix for qRT-PCR; Invitrogen). Expression of α1(I) procollagen mRNA was analyzed by quantitative reverse transcription-PCR (LightCycler; Roche Diagnostics Corporation, Indianapolis, IN). mRNA expression was normalized to the expression of β-actin. Primer sequences are as follows: α1(I) procollagen forward TGCTGCCTTTTCTGTTCCTT and reverse AAGGTGCTGGGTAGGGAAGT, and β-actin forward AGCCATGTACGTAGCCATCC and reverse CTCTCAGCTGTGGTGGTGAA. All reactions were performed in duplicate and the experiment was repeated to ensure reproducible results.

Statistics

All data are shown as mean ± SEM. Differences between two groups were tested with unpaired Student's t-Test with $p<0.05$ considered as significant.

Results

Characterization of animal models

Weekly treatment of rats with 100 mg/kg of DEN resulted in moderate to advanced fibrosis (individual Ishak scores 3–6) after 4 weeks. Morphological changes in the livers of DEN-treated animals were readily apparent (Fig. S1). Masson's trichrome staining revealed multiple portal fibrotic expansions with bridging fibrosis in livers of DEN-treated rats (Fig. 1A). Livers from control animals showed no noticeable fibrosis. Specific staining for collagen type I confirmed significant deposition in the DEN-treated livers compared to controls (Fig. 1B). Consistent with this, real-time PCR analysis of liver tissue confirmed that expression of α1(I) procollagen mRNA was 15-fold higher ($p<0.05$) in the fibrotic group compared to controls (Fig. 1C). Quantitative analysis of hydroxyproline (Hyp) was used as a

measure of the total amount of collagen in tissue. Hydroxyproline levels in fibrotic livers were on average 2.5-fold higher than in normal livers (control: 208±20, DEN: 528±72 μg Hyp/g liver, $p < 0.05$, Fig. 1D). As suggested by the error bars in Fig. 1D, inter-individual variations in hydroxyproline were somewhat higher in the fibrotic group than in the control group. This is consistent with the variations in Ishak scores and likely it is a result of individual sensitivities of animals to chronic liver injury. Together, these results demonstrate that the DEN model successfully induces fibrosis in rat liver accompanied by excessive deposition of collagen, including type I, in the extracellular matrix.

Similarly, after 20 weeks of oral CCl4 administration in mice, liver fibrosis reached a moderate to advanced stage (Ishak 3–6). Macroscopic changes in liver appearance were visible in all fibrotic specimens (Fig. S2A). In some cases we detected hepatocellular carcinomas that varied in size and quantity. Histology showed numerous portal fibrotic expansions with bridging in CCl4-treated livers, whereas there was no detectable fibrosis in the controls (Fig. S2B). Type I collagen immunostaining was markedly increased within the fibrotic regions of CCl4-treated livers compared to controls (Fig. S2C), and expression of α1(I) procollagen mRNA was significantly enhanced in fibrotic livers compared to controls (23-fold, $p < 0.05$, Fig. S2D). Total collagen was increased more than 2-fold in fibrotic livers as compared to controls (control: 191±5 μg Hyp/g, CCl4: 415±31 μg Hyp/g, $p < 0.01$, Fig. S2E). Hydroxyproline levels showed a uniform distribution among different lobes of each liver with a mean relative standard deviation of 15%, confirming that CCl4 treatment leads to a diffuse fibrotic response throughout the whole liver. In general, the CCl4 mouse model presented with a fibrosis that was similar to the rat DEN model.

MR imaging of liver fibrosis

We reasoned that immediately after injection, the contrast agent would be in excess in both the circulation and liver sinusoids relative to the concentration of collagen, and there may be little or no difference in intensity between fibrotic animals and controls. However as the contrast agent clears the systemic circulation, we expect to see differences between the fibrotic and control livers for the collagen-targeted agent EP-3533. In controls, where there are lower collagen levels, EP-3533 would wash out rapidly, but in fibrotic liver a fraction of the contrast agent would be bound to the elevated levels of collagen resulting in prolonged signal enhancement and slower liver signal washout. We would expect untargeted Gd-DTPA to show no difference in liver signal enhancement and washout between controls and fibrotic animals. Since the kinetics of liver washout with EP-3533 was unknown, T1 measurements and T1-weighted imaging were performed prior to, and at multiple time points out to one hour post injection.

Injection of contrast agents (either Gd-DTPA or EP-3533) led to shortening of T1 relaxation times in both normal and fibrotic livers (Fig. 2A). This resulted in positive signal enhancement in the liver but little/no change in the stomach or skeletal muscle signal post injection. To quantify the amount of probe *in vivo* we determined the T1 values in liver pre- and post-injection and calculated ΔR1 values. Since ΔR1 is linearly proportional to the probe concentration in tissue, we could determine the wash-out rate of the probe from liver (half-life, $t_{1/2}$) by analyzing changes in ΔR1. EP-3533 $t_{1/2}$ in fibrotic liver was significantly longer than in normal liver in both the rat and mouse models (rats: control = 42.0±2.5 min, DEN = 51.3±3.6 min, $p < 0.05$, Fig. 2B; mice: control = 44.1±2.9 min, CCl4 = 54.5±1.9 min, $p < 0.01$, Fig. S3B). There was no significant difference in Gd-DTPA half-lives between control and fibrotic livers in mice or rats (rats: control = 24.7±3.4 min, DEN = 20.7±8.0 min, $p = 0.33$, Fig. 2C; mice: control = 19.3±3.5 min, CCl4 = 14.6±0.8 min, $p = 0.14$, Fig. S3C). Baseline T1 values could not distinguish fibrosis in either model (rats: control = 785±58 ms, DEN = 803±35 ms, $p = 0.40$; mice: control = 971±18 ms, CCl4 = 990±23, $p = 0.26$).

In the initial rat study, we noted that although the $t_{1/2}$ of EP-3533 in the fibrotic livers was significantly longer than in control livers, single measures of signal change like ΔR1 were not significantly different between the two groups. This was traced to the small sample size, but also to experimental variability in the injected dose volume. As a result, the peak signal enhancement varied. For the mouse study, the protocol was expanded to include a dynamic study that allowed us to examine the signal enhancement in liver immediately after injection of the contrast agent, and to precisely measure peak enhancement. After EP-3533 injection, the CCl4-treated mice and the controls showed distinct differences in liver signal enhancement as demonstrated in Figure 3. The maximum enhancement was notably shifted towards later time points in the CCl4 group compared to controls (time-to-peak values, control: 27.2±5.5 s, CCl4: 93.0±17.1 s, p <0.01, Fig. 3A). After the initial liver enhancement, the two groups of animals quickly separated with respect to their signal enhancement values, with the CCl4 group showing slower signal washout resulting in higher signal enhancement at later time points (Fig. 3B). For example at 55 minutes post injection, the MR signal intensity in fibrotic mice was 41% higher than in the controls (control: 0.39±0.04, CCl4: 0.55±0.03, p <0.01). Gd-DTPA enhanced MRI showed no significant difference between the groups in terms of liver uptake (time-to-peak values, control: 27.0±4.3 s, CCl4: 33.0±2.5 s, p = 0.14, Fig. 3C), or wash-out (Fig. 3D).

The concentration of probe in rat liver was determined by elemental analysis *ex vivo* at 120 min after injection of EP-3533. The dose retained at this time point was on average 1.7-times higher in fibrotic livers compared to controls (control: 0.50±0.03 %ID/g, DEN: 0.82±0.06 %ID/g, p <0.001, Fig. 2D; %ID/g = percent of injected dose per gram liver). In mice, at 80 min after EP-3533 injection the liver/blood ratio in fibrotic animals was 1.5-times higher than in control animals (p <0.01, Fig. S3D). Analysis of mouse or rat liver either 24 or 48 hrs post Gd-DTPA confirmed that negligible residual Gd remained at this timepoint, in agreement with literature [32].

Correlation of MRI biomarkers with ex vivo analyses

In both animal models there were marked differences between fibrotic liver and normal liver in terms of EP-3533 half-lives and *ex vivo* hydroxyproline and gadolinium concentrations. We further investigated correlations between the *ex vivo* data and the imaging results. First, we validated that ΔR1 can serve as a reliable measure of EP-3533 concentration *in vivo*. Plots of the last measured ΔR1 vs. *ex vivo* gadolinium concentration showed very strong linear dependence in the CCl4 mouse model (r = 0.90, Fig. 4A; rats: r = 0.96, data not shown). This allowed us to estimate the relaxivity of EP-3533 in mouse liver as 17.1 $mM^{-1}s^{-1}$ and 16.2 $mM^{-1}s^{-1}$ in rat liver (4.7 T, 37 °C).

Next, we compared hydroxyproline and gadolinium concentrations in liver tissue and found a strong positive correlation in both animal models (mice: r = 0.77, Fig. 4B; rats: r= 0.74, data not shown). This strong association between collagen and gadolinium suggests that the higher retention of EP-3533 in fibrotic liver is likely caused by binding to over-expressed collagen. The half-life of EP-3533 in the liver as assessed by MRI showed moderately strong correlations with the total collagen (hydroxyproline) in both models (mice: r = 0.61, Fig. 4C; rats: r = 0.58, data not shown).

The basis of our hypothesis is that total liver collagen concentration correlates with the extent of fibrosis, and thus MR imaging of collagen is a direct measure of extent of fibrosis. Total collagen as measured by hydroxyproline analysis correlated well with the Ishak score (mice: r = 0.89, Fig. 4D; rats: r = 0.89), confirming that increasing fibrosis is associated with increased total collagen. There was also a strong positive correlation between gadolinium concentration and Ishak score (mice: r = 0.79, Fig. 4E; rats: r = 0.84, data not shown), or

liver half-life of EP-3533 and Ishak score (mice: $r = 0.64$; rats: $r = 0.81$, data not shown) demonstrating the feasibility of EP-3533 to quantify fibrosis.

Discussion

Liver fibrosis and its end-stage, cirrhosis, represent the final common pathway of virtually all chronic liver diseases [2]. While fibrosis can be identified and quantified using biopsy, repeated biopsy is not a practical solution for monitoring disease progression or response to therapy. Numerous noninvasive but indirect approaches have been taken to stage fibrosis. Blood biomarker panels, elastography, and certain MRI measurements (e.g. apparent diffusion coefficient) correlate with extent of fibrosis. However because of their indirect relationship to fibrosis, the readouts in these techniques can be altered by factors other than fibrosis. In theory, a direct measure of fibrosis should be more accurate than these correlative approaches.

In liver biopsy, collagen deposition is assessed histologically by staining (e.g. Masson's trichrome). Stained sections from liver biopsies can be semi-quantitatively scored, for example by the criteria of Ishak [30]. By analogy, we reasoned that molecular imaging of collagen would represent a direct and objective measure of fibrosis. The MRI probe EP-3533 was derived from a phage display screen against type I collagen and was previously shown to be effective and specific for identifying cardiac fibrosis in myocardial scar [28].

Liver MRI following EP-3533 administration showed slower signal washout from fibrotic animals compared to controls. This difference in $t_{1/2}$ led to stronger signal enhancement in fibrotic animals compared to controls at later time points. On the other hand, baseline imaging or Gd-DTPA enhanced MRI could not distinguish fibrotic animals from controls. Supportive of these findings were *ex vivo* analyses that showed strong correlations between probe and collagen concentrations. Similar results were observed in both the rat DEN model and the mouse CCl4 model suggesting the utility of molecular MR imaging of collagen for visualizing fibrosis.

MRI is a useful tool for characterizing liver disease. It is noninvasive, has deep tissue penetration, high spatial resolution, and does not involve ionizing radiation. The absence of ionizing radiation is particularly relevant in monitoring chronic disease where the patient may undergo numerous scans over a period of years. A further benefit of MRI is the ability to examine the whole organ compared to biopsy where only a small fraction of the organ is sampled.

MRI has been extensively investigated as a tool for detection of liver fibrosis [33, 34]. Measures of native MRI contrast have been evaluated in the context of fibrosis, including relaxation in the rotating frame (T1ρ) [26], magnetization transfer [35], and apparent diffusion coefficient (ADC) [36, 37]. Contrast-enhanced techniques utilizing clinically approved MR contrast agents have been reported as well [38–40]. Common to these approaches is that the imaging biomarkers are related to fibrosis rather indirectly and may be affected by other factors such as inflammation, liver perfusion and loss of hepatocyte function. The molecular imaging approach described here could be complementary to these existing MR techniques in order to bring more specificity with respect to the fibrotic component of the disease. We also note that MR can be used to quantify hepatic fat [41], and one can envision an MR protocol that reports on levels of collagen and fat.

While we have demonstrated the feasibility of collagen-targeted molecular imaging for identification of fibrosis, there are some limitations to the current study. First, the study was not powered to address the question of whether EP-3533 enhanced MRI could stage fibrosis.

Here, a chemical toxin was administered for a constant, fixed duration but this resulted in varying fibrosis with Ishak scores ranging from 3 to 6. The Ishak score represents pathological analysis on a very small sample of the liver, while the MR measurement is averaged over a large cross-section of the liver so there may be some discordance between these two measures. Future studies should be powered to examine the efficacy of the contrast agent over a range of Ishak scores, and the intrahepatic variability in Ishak score should be assessed. Second, the dose of EP-3533 used was not optimized and the sensitivity of the technique may be increased through dose optimization. Finally, our studies were performed using a high field (4.7T) small animal scanner. The relaxivity (MR efficiency) of EP-3533 is 3-fold lower at 4.7T compared to the common clinical field strength of 1.5T [27]. Thus the sensitivity of the probe to detect changes in liver collagen concentrations may be much higher when measured with a clinical MR scanner. Future work will address these questions of experimental optimization and fibrosis staging.

In conclusion, we demonstrate that MRI with a type I collagen-targeted probe can distinguish liver fibrosis in two animal models of disease. This molecular MR imaging technique, alone or in combination with other MRI techniques, offers the potential of directly imaging collagen and staging liver fibrosis.

Supplementary Material

Refer to Web version on PubMed Central for supplementary material.

Acknowledgments

Financial support: Grant numbers CA140861 (B.C.F.), CA009502 (G.S.L), CA076183 (K.K.T), and EB009062 (P.C.) from the National Cancer Institute and the National Institute of Biomedical Imaging and Bioengineering, and Tucker Gosnell Research funds (K.K.T.)

List of abbreviations

MRI	magnetic resonance imaging
MR	magnetic resonance
DTPA	diethylenetriaminepentaacetic acid
ECM	extra-cellular matrix
DEN	diethylnitrosamine
CCl4	carbon tetrachloride
RARE	rapid acquisition with refocused echoes
TR	repetition time
TE	echo time
FOV	field of view
DCE	dynamic contrast enhancement
HPLC	high performance liquid chromatography
ICP-MS	inductively coupled plasma-mass spectrometry
PCR	polymerase chain reaction
RNA	ribonucleic acid

cDNA	complementary deoxyribonucleic acid
mRNA	messenger ribonucleic acid
SEM	standard error of the mean
Hyp	hydroxyproline
ID	injected dose
T1ρ	longitudinal relaxation time in the rotating frame
ADC	apparent diffusion coefficient

References

1. Iredale JP. Models of liver fibrosis: exploring the dynamic nature of inflammation and repair in a solid organ. J Clin Invest. 2007; 117:539–548. [PubMed: 17332881]
2. Friedman SL. Mechanisms of hepatic fibrogenesis. Gastroenterology. 2008; 134:1655–1669. [PubMed: 18471545]
3. Bataller R, Brenner DA. Liver fibrosis. J Clin Invest. 2005; 115:209–218. [PubMed: 15690074]
4. Hui JM, Kench JG, Chitturi S, Sud A, Farrell GC, Byth K, et al. Long-term outcomes of cirrhosis in nonalcoholic steatohepatitis compared with hepatitis C. Hepatology. 2003; 38:420–427. [PubMed: 12883486]
5. Ratziu V, Bonyhay L, Di Martino V, Charlotte F, Cavallaro L, Sayegh-Tainturier MH, et al. Survival, liver failure, and hepatocellular carcinoma in obesity-related cryptogenic cirrhosis. Hepatology. 2002; 35:1485–1493. [PubMed: 12029634]
6. Williams R. Global challenges in liver disease. Hepatology. 2006; 44:521–526. [PubMed: 16941687]
7. Lavanchy D. Worldwide epidemiology of HBV infection, disease burden, and vaccine prevention. J Clin Virol. 2005; 34 (Suppl 1):S1–3. [PubMed: 16461208]
8. Wright TL. Introduction to chronic hepatitis B infection. Am J Gastroenterol. 2006; 101 (Suppl 1):S1–6. [PubMed: 16448446]
9. Fallowfield JA, Kendall TJ, Iredale JP. Reversal of fibrosis: no longer a pipe dream? Clin Liver Dis. 2006; 10:481–497. viii. [PubMed: 17162224]
10. Manning DS, Afdhal NH. Diagnosis and quantitation of fibrosis. Gastroenterology. 2008; 134:1670–1681. [PubMed: 18471546]
11. Ratziu V, Charlotte F, Heurtier A, Gombert S, Giral P, Bruckert E, et al. Sampling variability of liver biopsy in nonalcoholic fatty liver disease. Gastroenterology. 2005; 128:1898–1906. [PubMed: 15940625]
12. Afdhal NH, Nunes D. Evaluation of liver fibrosis: a concise review. Am J Gastroenterol. 2004; 99:1160–1174. [PubMed: 15180741]
13. Myers RP, Fong A, Shaheen AA. Utilization rates, complications and costs of percutaneous liver biopsy: a population-based study including 4275 biopsies. Liver Int. 2008; 28:705–712. [PubMed: 18433397]
14. Thampanitchawong P, Piratvisuth T. Liver biopsy:complications and risk factors. World J Gastroenterol. 1999; 5:301–304. [PubMed: 11819452]
15. Schmeltzer PA, Talwalkar JA. Noninvasive tools to assess hepatic fibrosis: ready for prime time? Gastroenterol Clin North Am. 2011; 40:507–521. [PubMed: 21893271]
16. Martinez SM, Crespo G, Navasa M, Forns X. Noninvasive assessment of liver fibrosis. Hepatology. 2011; 53:325–335. [PubMed: 21254180]
17. Clark PJ, Patel K. Noninvasive tools to assess liver disease. Curr Opin Gastroenterol. 2011; 27:210–216. [PubMed: 21248634]
18. Baranova A, Lal P, Birerdinc A, Younossi ZM. Non-Invasive markers for hepatic fibrosis. BMC Gastroenterol. 2011; 11:91. [PubMed: 21849046]

19. Cohen EB, Afdhal NH. Ultrasound-based hepatic elastography: origins, limitations, and applications. J Clin Gastroenterol. 2010; 44:637–645. [PubMed: 20844365]
20. Cobbold JF, Morin S, Taylor-Robinson SD. Transient elastography for the assessment of chronic liver disease: ready for the clinic? World J Gastroenterol. 2007; 13:4791–4797. [PubMed: 17828808]
21. Rockey DC. Noninvasive assessment of liver fibrosis and portal hypertension with transient elastography. Gastroenterology. 2008; 134:8–14. [PubMed: 18166342]
22. Friedrich-Rust M, Ong MF, Martens S, Sarrazin C, Bojunga J, Zeuzem S, et al. Performance of transient elastography for the staging of liver fibrosis: a meta-analysis. Gastroenterology. 2008; 134:960–974. [PubMed: 18395077]
23. Mariappan YK, Glaser KJ, Ehman RL. Magnetic resonance elastography: a review. Clin Anat. 2010; 23:497–511. [PubMed: 20544947]
24. Rouviere O, Yin M, Dresner MA, Rossman PJ, Burgart LJ, Fidler JL, et al. MR elastography of the liver: preliminary results. Radiology. 2006; 240:440–448. [PubMed: 16864671]
25. Huwart L, Sempoux C, Vicaut E, Salameh N, Annet L, Danse E, et al. Magnetic resonance elastography for the noninvasive staging of liver fibrosis. Gastroenterology. 2008; 135:32–40. [PubMed: 18471441]
26. Wang Y, Ganger DR, Levitsky J, Sternick LA, McCarthy RJ, Chen ZE, et al. Assessment of chronic hepatitis and fibrosis: comparison of MR elastography and diffusion-weighted imaging. AJR Am J Roentgenol. 2011; 196:553–561. [PubMed: 21343496]
27. Caravan P, Das B, Dumas S, Epstein FH, Helm PA, Jacques V, et al. Collagen-targeted MRI contrast agent for molecular Imaging of fibrosis. Angewandte Chemie-International Edition. 2007; 46:8171–8173.
28. Helm PA, Caravan P, French BA, Jacques V, Shen L, Xu Y, et al. Postinfarction myocardial scarring in mice: molecular MR imaging with use of a collagen-targeting contrast agent. Radiology. 2008; 247:788–796. [PubMed: 18403626]
29. Rohrer M, Bauer H, Mintorovitch J, Requardt M, Weinmann HJ. Comparison of magnetic properties of MRI contrast media solutions at different magnetic field strengths. Invest Radiol. 2005; 40:715–724. [PubMed: 16230904]
30. Ishak K, Baptista A, Bianchi L, Callea F, De Groote J, Gudat F, et al. Histological grading and staging of chronic hepatitis. J Hepatol. 1995; 22:696–699. [PubMed: 7560864]
31. Hutson PR, Crawford ME, Sorkness RL. Liquid chromatographic determination of hydroxyproline in tissue samples. Journal of Chromatography B-Analytical Technologies in the Biomedical and Life Sciences. 2003; 791:427–430.
32. Tweedle MF, Wedeking P, Kumar K. Biodistribution of radiolabeled, formulated gadopentetate, gadoteridol, gadoterate, and gadodiamide in mice and rats. Invest Radiol. 1995; 30:372–380. [PubMed: 7490190]
33. Taouli B, Ehman RL, Reeder SB. Advanced MRI methods for assessment of chronic liver disease. AJR Am J Roentgenol. 2009; 193:14–27. [PubMed: 19542391]
34. Talwalkar JA, Yin M, Fidler JL, Sanderson SO, Kamath PS, Ehman RL. Magnetic resonance imaging of hepatic fibrosis: emerging clinical applications. Hepatology. 2008; 47:332–342. [PubMed: 18161879]
35. Kim H, Booth CJ, Pinus AB, Chen P, Lee A, Qiu M, et al. Induced hepatic fibrosis in rats: hepatic steatosis, macromolecule content, perfusion parameters, and their correlations--preliminary MR imaging in rats. Radiology. 2008; 247:696–705. [PubMed: 18403622]
36. Taouli B, Koh DM. Diffusion-weighted MR imaging of the liver. Radiology. 2010; 254:47–66. [PubMed: 20032142]
37. Fujimoto K, Tonan T, Azuma S, Kage M, Nakashima O, Johkoh T, et al. Evaluation of the mean and entropy of apparent diffusion coefficient values in chronic hepatitis C: correlation with pathologic fibrosis stage and inflammatory activity grade. Radiology. 2011; 258:739–748. [PubMed: 21248235]
38. Aguirre DA, Behling CA, Alpert E, Hassanein TI, Sirlin CB. Liver fibrosis: noninvasive diagnosis with double contrast material-enhanced MR imaging. Radiology. 2006; 239:425–437. [PubMed: 16641352]

39. Tamada T, Ito K, Higaki A, Yoshida K, Kanki A, Sato T, et al. Gd-EOB-DTPA-enhanced MR imaging: Evaluation of hepatic enhancement effects in normal and cirrhotic livers. Eur J Radiol. 2011; 80:e311–316. [PubMed: 21315529]

40. Watanabe H, Kanematsu M, Goshima S, Kondo H, Onozuka M, Moriyama N, et al. Staging hepatic fibrosis: comparison of gadoxetate disodium-enhanced and diffusion-weighted MR imaging--preliminary observations. Radiology. 2011; 259:142–150. [PubMed: 21248234]

41. Reeder SB, Cruite I, Hamilton G, Sirlin CB. Quantitative assessment of liver fat with magnetic resonance imaging and spectroscopy. J Magn Reson Imaging. 2011; 34:729–749. [PubMed: 21928307]

42. Kiryu S, Inoue Y, Yoshikawa K, Shimada M, Watanabe M, Ohtomo K. Diet and gastrointestinal signal on T1-weighted magnetic resonance imaging of mice. Magn Reson Imaging. 2010; 28:273–280. [PubMed: 20061108]

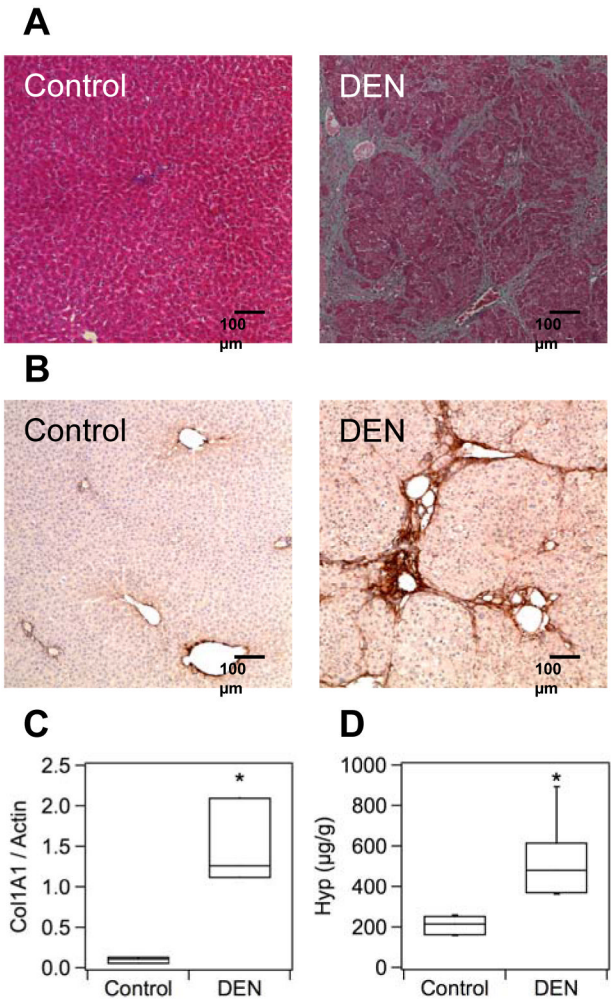

Fig. 1. Characterization of fibrosis and collagen deposition in the rat DEN model

(A) Masson's trichrome staining reveals numerous portal fibrotic expansions in the DEN sample corresponding to advanced fibrosis, Ishak 5 in this example. There is no detectable fibrosis in the control sample. (B) Immunostaining for type I collagen in liver shows rich staining in the DEN treated animals but is absent in the controls. (C) Expression of liver α1(I) procollagen mRNA was 15-fold higher (* p <0.05) in the DEN treated group compared to controls. (D) Total liver collagen (as hydroxyproline) is 2.5-fold higher in DEN treated animals compared to controls (* p <0.05). Box plots in Panels (C) and (D) illustrate median (line inside box), interquartile range (box), and minimal and maximal (lines extending above and below box) values.

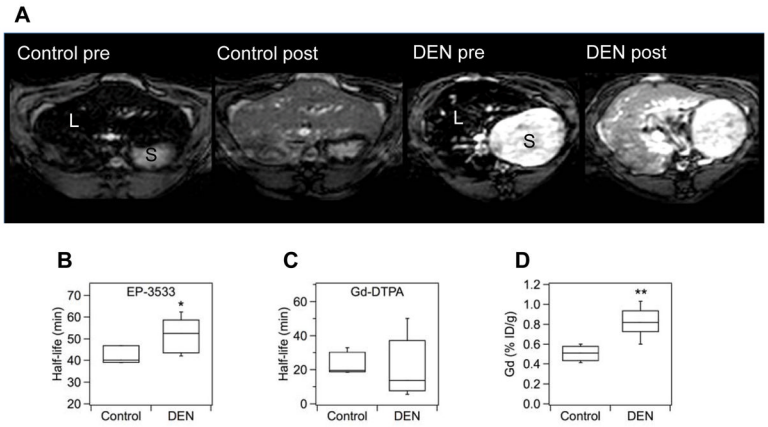

Fig. 2. MR imaging of liver fibrosis in the rat DEN model

(A) Inversion recovery MRI (TR/TE/TI=3200ms/4ms/507ms) of rat liver before and 40 min after injection of 20 μmol/kg EP-3533; S = stomach, L = liver. The inversion time was chosen to minimize liver signal prior to probe injection. Post injection there is higher signal in the liver of the DEN treated animal compared to the control. Differences in baseline stomach signal are due to the absence/presence of chow which shortens stomach T1 [42]. (B) EP-3533 was retained longer in fibrotic livers than in controls (* $p < 0.05$), while (C) the half-life of Gd-DTPA in the liver did not statistically differ between DEN and control groups. (D) Ex vivo analysis of EP-3533 (as gadolinium) at 120 min post injection showed 70% higher gadolinium levels in the DEN group compared to controls (** $p < 0.01$).

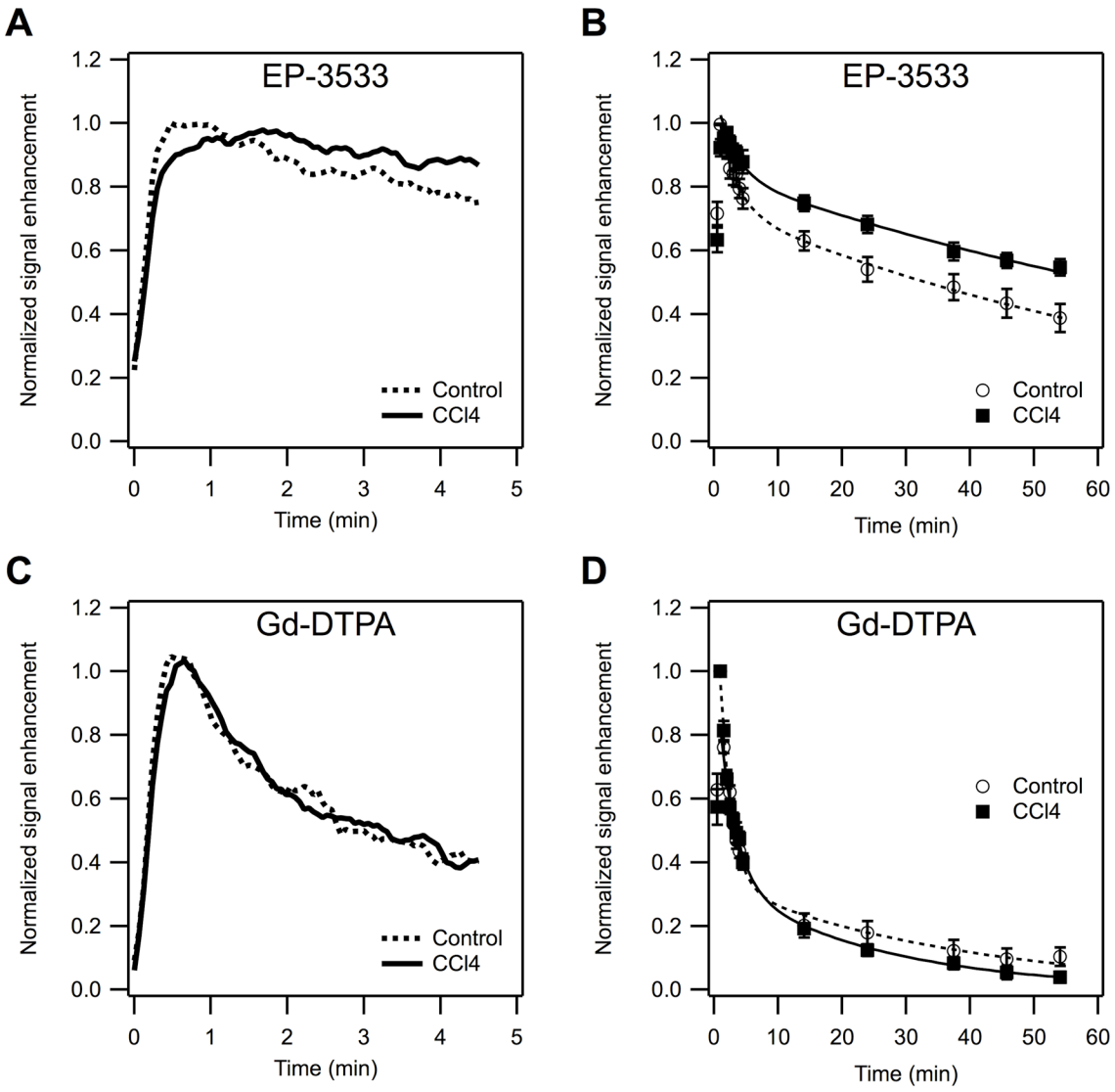

Fig. 3. Dynamic MR enhancement of the liver in CCl4 treated and control mice

Dynamic MRI (TR/TE/flip angle=50ms/1.92ms/35°) after injection of either collagen-binding EP-3533 or non-specific Gd-DTPA probe normalized to peak signal enhancement. (A, C) Expansion of first 4.5 min after injection showing that with EP-3533 (A), the peak enhancement appears later and the wash-out is slower in the CCl4 group compared to control, but Gd-DTPA (C) shows no noticeable difference between the control and fibrotic groups. (B, D) Complete signal enhancement profiles out to 60 min post injection. EP-3533 (B) shows slower liver wash-out from CCl4 animals compared to controls resulting into higher relative signal enhancement at later time points. Gd-DTPA (D) does not show significant differences between the two groups.

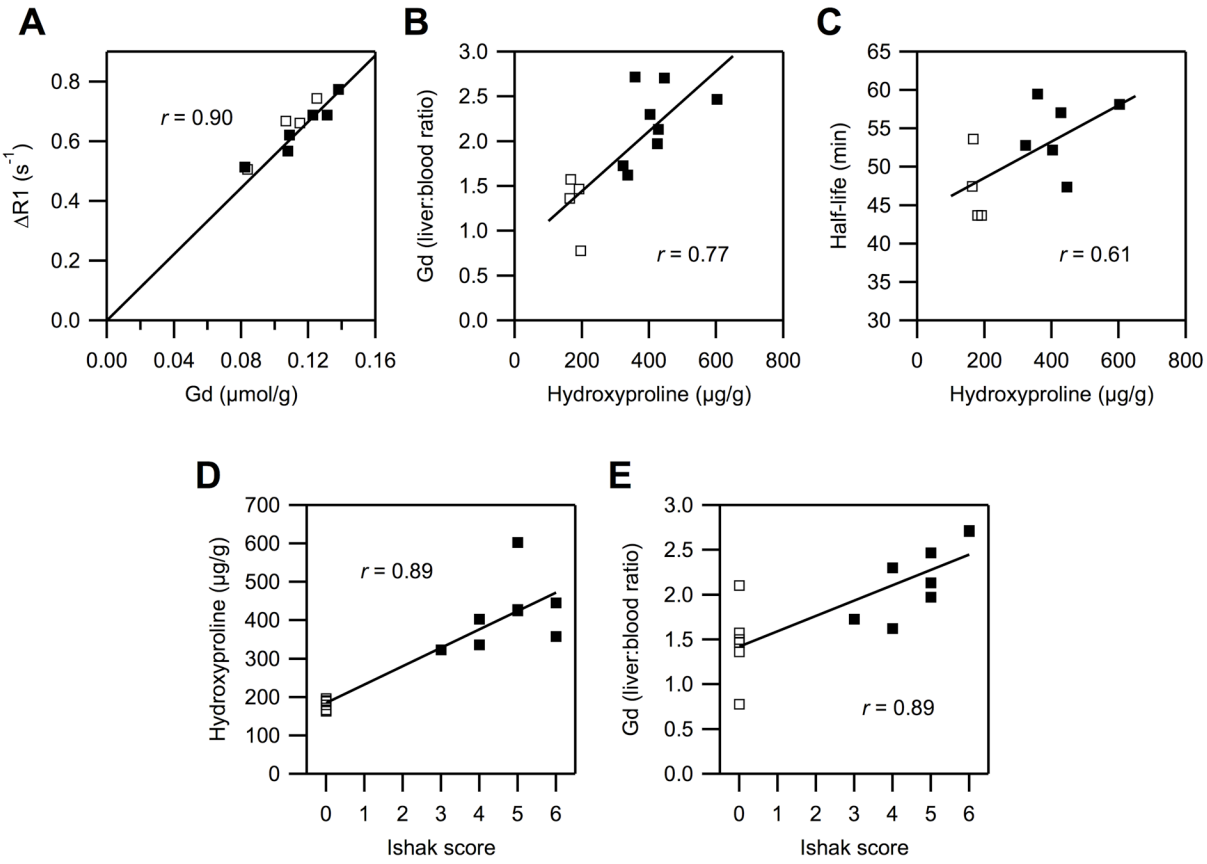

Fig. 4. Correlations between MRI and *ex vivo* analyses

Open squares: controls, filled squares: CCl4 treated animals. (A) Gadolinium in liver at 80 min after EP-3533 injection correlates linearly with relaxation rate enhancement (ΔR1) observed at 60 min. (B) Gadolinium (EP-3533) liver:blood ratios correlate with hydroxyproline (total collagen), showing an association of the probe with increased collagen levels. (C) Half-life of EP-3533 in the liver as determined by MRI correlates with total collagen, showing the feasibility of molecular MR imaging to detect fibrosis. (D) Increasing stage of fibrosis (Ishak score) is well reflected in the increase of hydroxyproline concentration in tissue. (E) Probe uptake into liver (gadolinium liver:blood) increases with increasing stage of fibrosis.